

This discussion paper is/has been under review for the journal Earth Surface Dynamics (ESurfD).  
Please refer to the corresponding final paper in ESurf if available.

# Observations of the effect of emergent vegetation on sediment resuspension under unidirectional currents and waves

**R. O. Tinoco and G. Coco**

Environmental Hydraulics Institute IH Cantabria, University of Cantabria, Santander, Spain

Received: 10 October 2013 – Accepted: 15 October 2013 – Published: 28 October 2013

Correspondence to: R. O. Tinoco (tinocor@unican.es)

Published by Copernicus Publications on behalf of the European Geosciences Union.

## Observations of the effect of emergent vegetation

R. O. Tinoco and G. Coco

Title Page

Abstract

Introduction

Conclusions

References

Tables

Figures

⏪

⏩

◀

▶

Back

Close

Full Screen / Esc

Printer-friendly Version

Interactive Discussion





tidal areas, forms a network of pneumatophores, protruding through the water surface to allow for root respiration (Houck and Neill, 2009), forming an array that shelters the sediment and organisms around it.

The effects of such populations on sediment resuspension and deposition as a function of the properties of the array (i.e. density, porosity, solid volume fraction, individual spacing) are still not well understood (Eckman et al., 1981; Carey, 1983; Luckenbach, 1986; Graf and Rosenberg, 1997; Friedrichs et al., 2000; Coco et al., 2006), and one even finds contradictory results between field and experimental studies (Madsen et al., 2001), which emphasizes the need to distinguish between purely physical effects, as the ones we address, and purely biological effects, as the ones generated by macrophytes, microphytobenthos or macrofauna (LeHir et al., 2007). For example: an increase in turbulence by the physical presence of benthic organisms may enhance resuspension, but the mucus produced by those same organisms can form a protective film that suppresses it.

As Nikora (2010) points out, the growing new field of hydrodynamics of aquatic ecosystems needs to eliminate the multiple knowledge gaps between fluid mechanics, ecology and biomechanics. The work presented herein adds another step, by incorporating biomorphodynamics into a broader picture.

### 1.1 Thresholds of sediment motion for a flat, sandy bed

There are many studies on critical stresses and velocities for sediment motion and resuspension on a flat, sandy bed under currents and waves. However, literature on thresholds of motion for sediment within patches of vegetation or benthic populations is very scarce. We present herein a few of the existing criteria describing critical velocities and critical bed shear-stress for sediment motion, as well as critical velocities for resuspension. While those refer to non-populated beds, they will offer a good starting point for comparison against the results from populated cases, allowing us to investigate the impact of the added physical processes within a patch of vegetation.

## Observations of the effect of emergent vegetation

R. O. Tinoco and G. Coco

Title Page

Abstract

Introduction

Conclusions

References

Tables

Figures



Back

Close

Full Screen / Esc

Printer-friendly Version

Interactive Discussion



## Observations of the effect of emergent vegetation

R. O. Tinoco and G. Coco

Title Page

Abstract

Introduction

Conclusions

References

Tables

Figures

◀

▶

◀

▶

Back

Close

Full Screen / Esc

Printer-friendly Version

Interactive Discussion



### a. Critical velocities:

From VanRijn (1984):

$$U_{cr} = 0.19d_{50}^{0.1} \log_{10} (4D/d_{90}) ; 100 < d_{50} < 500 \mu\text{m}$$

$$U_{cr} = 8.5d_{50}^{0.6} \log_{10} (4D/d_{90}) ; 500 < d_{50} < 2000 \mu\text{m}$$

where  $D$  is the water depth, and  $d_{50}$  and  $d_{90}$  are the correspondent percentiles on the granulometric curve.

From Soulsby (1997):

$$U_{cr} = 7 \left( \frac{D}{d_{50}} \right)^{1/7} [g(s_{\rho} - 1)d_{50}f(D_*)]^{1/2}$$

where

$$s_{\rho} = \frac{\rho_s}{\rho} = \frac{\text{density of the sediment}}{\text{density of the fluid}}$$

$$D_* = \left( \frac{g(s_{\rho} - 1)}{v^2} \right)^{1/3} d_{50}$$

$$f(D_*) = \frac{0.30}{1 + 1.2D_*} + 0.055 \left( 1 - e^{-0.020D_*} \right)$$

and  $g$  is gravity, for values of  $D_* > 0.1$ .

## Observations of the effect of emergent vegetation

R. O. Tinoco and G. Coco

Title Page

Abstract

Introduction

Conclusions

References

Tables

Figures

◀

▶

◀

▶

Back

Close

Full Screen / Esc

Printer-friendly Version

Interactive Discussion



### b. Critical bed shear-stress.

From Soulsby and Whitehouse (Soulsby, 1997) we get values for critical bed shear stress from the Shields curve, and Soulsby fit to the Shields curve as:

$$\theta_{\text{cr}} = \frac{0.24}{D_*} + 0.055 \left(1 - e^{-0.020D_*}\right)$$

$$\theta_{\text{cr}} = \frac{0.30}{1 + 1.2D_*} + 0.055 \left(1 - e^{-0.020D_*}\right)$$

where one can calculate:

$$\tau_{\text{cr}} = \theta_{\text{cr}} g (\rho_s - \rho) d_{50}$$

$$u_* = \left(\frac{\tau_{\text{cr}}}{\rho}\right)^{1/2}$$

such that a mean velocity can be estimated as:

$$U_{\text{cr}} = \frac{u_*}{\kappa} \ln\left(\frac{z}{z_0}\right)$$

using Kolmogorov's  $\kappa = 0.41$ , and estimating  $z_0$  from Nikuradse's roughness:

$$z_0 = \frac{k_s}{30} \left(1 - \exp\left[\frac{-u_* k_s}{27v}\right]\right) + \frac{v}{9u_*}$$

with  $k_s = 2.5d_{50}$ .

### c. Resuspension thresholds.

We use two criteria based on the settling velocity of the sand particles,  $w_s$ , given empirically for natural sands as (Soulsby, 1997):

$$w_s = \frac{v}{d_{50}} \left[ \left(10.36^2 + 1.049D_*^3\right)^{1/2} - 10.36 \right]$$

First, considering local turbulent bursts of sediment particles are lifted when (Van-Rijn, 1984):

$$u_{*cr} = \frac{4w_s}{D_*}, D_* < 10$$

$$u_{*cr} = 0.4w_s, D_* > 10$$

Second, assuming no material can be suspended unless the friction velocity exceeds the settling velocity (Soulsby, 1997):

$$u_* \geq w_s$$

In the case of waves, the wave-orbital velocity theory from Komar and Miller (1973) has been shown to give accurate predictions for sand resuspension (Green, 1999). A critical orbital velocity,  $U_{wc}$  can be calculated from:

$$\frac{\rho U_{wc}^2}{(\rho_s - \rho)gd_{50}} = 0.21 \left( \frac{d_w}{d_{50}} \right)^{1/2}$$

where  $d_w = \frac{U_{wc}T}{2\pi}$  is the near-bottom orbital excursion.

## 1.2 Studies on flow through aquatic vegetation

Several research groups have studied flow through aquatic vegetation. Nepf (2012a) summarizes some of the experimental work done on rigid and flexible, emergent and submerged model vegetation subject to unidirectional currents on a flat, rigid bed. Nepf (2012b) highlights the challenges on the study of vegetated flows, specifically mentioning the need for a better understanding of sediment motion processes within vegetated regions, pointing out that (a) there is no reliable method to estimate bed stresses within the vegetation, (b) it is not known if bed shear stress is the only relevant parameter,

### Observations of the effect of emergent vegetation

R. O. Tinoco and G. Coco

Title Page

Abstract

Introduction

Conclusions

References

Tables

Figures

◀

▶

◀

▶

Back

Close

Full Screen / Esc

Printer-friendly Version

Interactive Discussion





by a 2 m by 2 m piston-type wave maker with a maximum stroke of 2.0 m. Two agitators run in parallel to generate flow in the flume, and can be set independently to run at frequencies,  $f_p$ , between 20 and 50 Hz.

An 18 m long, 0.20 m deep, sand bed was built, where a 6 m long array of randomly placed, rigid cylinders was located, as shown in Fig. 2. Water depth was set at  $D = 0.16$  m, to ensure emergent conditions at all times during the waves series. The sediment is well-sorted,  $d_{50} = 0.31$  mm, silica sand.

PVC cylinders, with a diameter  $d = 0.02$  m, were used to represent on a 1 : 1 scale either populations of tube worms (e.g. *Sabella spallanzanii*) and mangrove roots (e.g. *Avicennia germinans*). The arrays were designed by defining the number of elements per square meter,  $n$ , and a minimum distance,  $s_{\min} = d$ , allowed between the edges of adjacent cylinders. Three densities were considered to represent a sparse, intermediate and dense population:  $n = \{25, 150, 250\} \text{ m}^{-2}$ . Three relevant parameters of the array are calculated for each density (1) volumetric frontal area of the array,  $a$  ( $\text{m}^{-1}$ ), given as the frontal area of the cylinders,  $A_f = N_{\text{cylinders}} dD$ , per volume,  $V = A_{\text{planform}} D$ , which reduces to  $a = nd$ , (2) solid volume fraction  $\phi$  ( ), given as the ratio between the volume of solids and fluid volume, or  $\phi = n\pi d^2/4$  for emergent cylinders, and (3) the mean separation between cylinders,  $\langle s \rangle$  (m), given in non-dimensional form as  $\langle s \rangle/d$  (Table 1). To ensure fully covering the range from sparse to dense conditions, the selected densities satisfy criteria proposed by Friedrichs et al. (2000), defining dense arrays as those with values of  $\phi > 0.045$ , and by Nepf (2012a), with sparse arrays for arrays with  $aD \ll 0.1$ , and considered dense if  $aD \gg 0.1$ . We chose the intermediate density,  $n = 150 \text{ m}^{-2}$  to be in the limit between sparse and rigid arrays.

Acoustic Doppler velocimeters (ADV – Nortek Vectrino) and optical backscatter sensors (OBS – Seapoint turbidity meter, SeaPoint Sensors Inc.), recording at a sampling frequency  $f_s = 50$  Hz, were used to measure synchronous records of velocities and concentrations, respectively. For the emergent case presented herein, ADVs and OBSs were located 5 cm above the sand bed, at the beginning ( $x_c = 0$  m) and at the middle

## Observations of the effect of emergent vegetation

R. O. Tinoco and G. Coco

Title Page

Abstract

Introduction

Conclusions

References

Tables

Figures



Back

Close

Full Screen / Esc

Printer-friendly Version

Interactive Discussion



( $x_c = 3$  m) of the array. A total of 19 capacitive wave gauges (Akamina technologies) were used for free surface measurements along the length of the flume.

For the study on unidirectional currents, different flow rates were ran for each array density, increasing the frequency of one of the flume agitators from  $f_p = 20$ –50 Hz. The range of velocities considered falls in a range of Reynolds numbers  $Re_D = UD/\nu < 4 \times 10^4$ , and  $Re_d = Ud/\nu < 5 \times 10^3$  for all cases. Flow remained subcritical, with  $Fr < 0.2$  for all cases.

For studies on waves, five cases with monochromatic waves were conducted for each density, with a constant period  $T = 2.5$  s and nominal wave height  $H = 0.01$ –0.05 m. For a water depth  $D = 0.16$  m, the dispersion relationship yields a wavelength  $\lambda = 3.08$  m, fitting two wavelengths within the 6 m array. Series of 50 waves were generated for each  $H$ . The maximum values presented are for  $H = 0.05$  m, given that breaking occurred at  $H = 0.06$  m.

### 3 Results

#### 3.1 Currents

For each density, the series was stopped once the velocities started causing large alterations in the bed (see Figs. 3 and 4). As seen in Fig. 5, as the density of the array increased, significant scour appeared for lower velocities, thus reducing the range of velocities studied for the denser cases (fewer data points for  $n = 250 \text{ m}^{-2}$  in Fig. 5).

Time averaged longitudinal,  $x$  velocities are shown in Fig. 5 (left) for the same flow conditions for each array density. The measured response by the OBS for all densities studied are also shown in Fig. 5 (right). We notice an abrupt jump in the concentration values for the two denser cases once a critical value is reached, in contrast with the trend seen for the non-populated case.

## Observations of the effect of emergent vegetation

R. O. Tinoco and G. Coco

Title Page

Abstract

Introduction

Conclusions

References

Tables

Figures

◀

▶

◀

▶

Back

Close

Full Screen / Esc

Printer-friendly Version

Interactive Discussion





flume were more evident at the non-populated case (noticed by the fluctuations in  $H_m$ ), since the cylinders were very efficient also at damping reflected waves.

While wave dissipation is not the main focus of our work, the effect of the array at dissipating the incoming waves is evident, with reductions of more than 50% of the approaching wave height for the densest cases (Fig. 8). With energy being dissipated as the wave advances through the array, the bottom shear stresses also decrease, reducing resuspension in favour of sediment deposition. Figures 9 and 10 show the up- and downstream edges of the array before and after a series of 50 waves. Scour and bedforms are clearly present at the upstream section, whereas the downstream area shows little, if any, bed disruptions. This behaviour is contrary to the one observed for currents, where the array effectively slows down the flow, yielding smaller velocities at the upstream section than at the downstream exit.

To account for the relationship between orbital velocities within the array and the measured concentrations, the maximum velocities in both directions ( $U_{w+}$  and  $U_{w-}$ ) were obtained from the records. The near-bottom orbital excursion,  $d_w = \frac{U_{w+} T}{2\pi}$ , was calculated using  $U_{w+}$  as the near-bottom orbital speed (Table 2). The relationship between the near bottom orbital speed and recorded values of suspended sediment concentration appears in Figs. 11 and 12. From the results from the station at  $x_c = 3$  m it is clear the difference between sparse ( $n = 0, 25 \text{ m}^{-2}$ ) and dense ( $n = 150, 250 \text{ m}^{-2}$ ) arrays, with the data almost collapsing into two distinctive curves in Fig. 12.

We also compare the behaviour of free surface elevation and concentration for the non-populated and the densest case, at the two instrumented locations (Figs. 13 and 14). The correlation between the time series is evident, and the amount of suspended sediment increases as the wave travels through the sand bed for  $n = 0$ , while the opposite occurs for the densest case. The effect was clearly visible during the experiments, with a cloud of sediment being lifted as the wave encountered the array.

To look at the correlation between the recorded velocities and concentrations, the frequency spectra are calculated for the  $n = 0$  and  $n = 250 \text{ m}^{-2}$  cases, as shown in Fig. 15.

## Observations of the effect of emergent vegetation

R. O. Tinoco and G. Coco

Title Page

Abstract

Introduction

Conclusions

References

Tables

Figures

◀

▶

◀

▶

Back

Close

Full Screen / Esc

Printer-friendly Version

Interactive Discussion



## 4 Discussion

### 4.1 Currents

The results present some clear trends relevant to the impact of benthos on sediment motion.

Even when longitudinal,  $x$  velocities are being damped by the presence of the array (Fig. 5), turbulent kinetic energy,  $k = \frac{1}{2} (u'^2 + v'^2 + w'^2)$ , is generated within the cylinders (Fig. 6), enhancing the resuspension process and accelerating the onset of sediment transport, consistent with the findings of Sumer et al. (2003), that observed significant increases in sediment transport if they increase turbulence levels while keeping the same flow speeds.

For the denser cases, even at low speeds, scour begins to occur, the wake behind each cylinder contributes to lifting the sediment, interacting with the adjacent wakes and the reduced current, allowing for the sediment to stay in suspension for the instruments to capture. Comparing Figs. 5 and 6, it is apparent that neither the mean flow speed, nor the turbulent kinetic energy, are the sole responsible for the resuspension: looking at Fig. 5 (right), lower values of  $k$  are required to reach similar values of  $C$  at  $n = 150 \text{ m}^{-2}$  than at  $n = 250 \text{ m}^{-2}$ , consistent with velocities within the  $n = 150 \text{ m}^{-2}$  array higher than those within the densest one. Follett and Nepf (2012) also noted the competing effect between the reduced velocities and increase of turbulent production as the density increases, resulting in increased scour at higher densities, concluding that given the small size of their patch ( $< 0.22 \text{ m}$ ), it behaved as the leading edge of a longer patch. However, our measurements at the middle of our array, where fully developed flow is expected, continue to show the same increase in scour.

As a reference point, we can compare the threshold values obtained from the OBS readings (Table 3) against theoretical values from non-populated mobile beds (see Sect. 1.1). The predicted values (Table 4) are considerably higher than the ones observed during the experiments, not only in the populated cases, where the cylinders

## Observations of the effect of emergent vegetation

R. O. Tinoco and G. Coco

Title Page

Abstract

Introduction

Conclusions

References

Tables

Figures

◀

▶

◀

▶

Back

Close

Full Screen / Esc

Printer-friendly Version

Interactive Discussion



clearly enhance sediment resuspension, but also in the smooth sand bed case, which can be explained either by irregularities in the flat initial conditions of the sand bed, or by the effect of the intrusive instrumentation deployed (steel rods protruding through the sand to hold ADVs and OBSs).

## 4.2 Waves

Data presented in Figs. 11 and 12 hint at a density independence within certain density ranges. Madsen et al. (2001) found contradictory results in studies arguing whether or not density is a relevant parameter for velocity reduction. Our data shows that (a) results depend significantly in the location of the measurement, and (b) density values within the same regime (sparse, intermediate or dense) can share similar behaviours, but the relevance of the density can not be overlooked (e.g. from Figs. 11 and 12, looking only at the results for  $n = 25$  and  $150 \text{ m}^{-2}$  the effect of density is clear, while looking only at the  $n = 250$  and  $150 \text{ m}^{-2}$  can mislead into conclusions of density independence).

The data presented in Fig. 12 allow us to estimate a critical orbital velocity for each density. We compare those values, presented in Table 3, against the theoretical threshold,  $U_{wc} = 0.112 \text{ m s}^{-1}$  from Komar and Miller (1973) for non-populated mobile beds. The measured values for the sparse cases,  $n = 0$  and  $n = 25 \text{ m}^{-2}$ , agree with the predicted value, while the densest cases show a near 40 % reduction of the critical velocity.

Additional effects of the array density were observed by looking at the spectra to investigate correlation between velocities and concentration. Figure 15 shows two relevant features: (1) the presence of higher frequency harmonics in all cases, (2) the smoother spectra for the densest case, with none of the large peaks observed in the non-populated case, showing a redistribution of energy within the array, with more energy contained at smaller scales and higher frequencies, and (3) the same redistribution appears as we move from  $x_c = 0$  to  $x_c = 3 \text{ m}$  through the array, with an evident shift in the energy cascade.

## Observations of the effect of emergent vegetation

R. O. Tinoco and G. Coco

Title Page

Abstract

Introduction

Conclusions

References

Tables

Figures

◀

▶

◀

▶

Back

Close

Full Screen / Esc

Printer-friendly Version

Interactive Discussion



## Observations of the effect of emergent vegetation

R. O. Tinoco and G. Coco

Title Page

Abstract

Introduction

Conclusions

References

Tables

Figures

◀

▶

◀

▶

Back

Close

Full Screen / Esc

Printer-friendly Version

Interactive Discussion



Madsen et al. (2001) found differences in the interactions between flow, vegetation and sediment, among regions dominated by either waves or unidirectional currents, finding contradictory results in (a) whether or not the density is relevant for velocity reduction, (b) if turbulence decreased or increased within vegetation, and (c) whether sediment resuspension is higher in wave-dominated areas than in tide-dominated ones. As pointed out through the present manuscript, one must be extremely cautious when comparing: (1) emergent and submerged conditions: the added mixing layer and the appearance of skimming flow in the submerged case produce contradictory results within the vegetation, (2) rigid and flexible model vegetation: plants bending under currents create a different and increased sheltering effect damping possible coherent structures that would appear on rigid structures, while the flapping of flexible vegetation under waves increases the bed exposition to the flow and changes the energy dissipation with respect to rigid element, (3) laboratory and field studies: although density effects on resuspension have already been reported (e.g. Widdows and Brinsley, 2002), it is worth reiterating that biological interactions in the field between the organisms and the sediment can produce an effect contrary to the expected from their physical presence (e.g. plants roots or biofilms holding the sediment together).

## 5 Conclusions

Arrays of randomly placed emergent cylinders, simulating benthic populations, change the flow-sediment interactions around and within the array.

The presence of arrays of rigid cylinders enhances sediment resuspension under waves and currents. The measured critical velocities for the densest cases are considerably smaller than those for the sparsest cases, and smaller than predicted velocities for non-populated beds.

With unidirectional currents, by slowing down the flow, emergent arrays might be expected to suppress bottom shear stress, reduce resuspension and favour deposition.

However, the cylinder wakes enhance scour, and the increased turbulence levels within the array effectively enhance resuspension.

For the sparse cases under currents, the values of suspended sediment concentration begin to increase slowly when the threshold is reached, as opposed to the dense cases where once the threshold is reached there is an abrupt jump in such values.

For both waves and currents, eddies break down to smaller scales as they move through the array, with energy passing from wave-scales to individual cylinder-scales.

The density of the array is a determining parameter on the early onset of sediment resuspension. There is a clear distinction between the resuspension behaviour of sparse and dense arrays, but it can not be interpreted as density independence.

More studies are needed to further improve understanding and predictive capability of resuspension in these fragile environments.

*Acknowledgements.* The authors gratefully acknowledge the support of the Augusto Gonzalez Linares program at the University of Cantabria.

## References

- Borsje, B., Kruijt, M., Werf, J., Hulscher, S., and Herman, P.: Modeling biogeomorphological interactions in underwater nourishments, Coastal Engineering Proceedings, 1, 2011. 607
- Bouma, T., van Duren, L., Temmerman, S., Claverie, T., Blanco-Garcia, A., Ysebaert, T., and Herman, P.: Spatial flow and sedimentation patterns within patches of epibenthic structures: Combining field, flume and modelling experiments, Cont. Shelf Res., 27, 1020–1045, 2007. 607
- Carey, D.: Particle resuspension in the benthic boundary layer induced by flow around polychaete tubes, Can. J. Fish. Aquat. Sci., 40, 301–308, 1983. 603
- Coco, G., Thrush, S., Green, M., and Hewitt, J.: Feedbacks between bivalve density, flow, and suspended sediment concentration on patch stable states, Ecology, 87, 2862–2870, 2006. 603
- Eckman, J., Nowell, A., and Jumars, P.: Sediment destabilization by animal tubes, J. Mar. Res., 39, 361–374, 1981. 603

# ESURFD

1, 601–636, 2013

## Observations of the effect of emergent vegetation

R. O. Tinoco and G. Coco

Title Page

Abstract

Introduction

Conclusions

References

Tables

Figures



Back

Close

Full Screen / Esc

Printer-friendly Version

Interactive Discussion



---

## Observations of the effect of emergent vegetation

R. O. Tinoco and G. Coco

---

Title Page

Abstract

Introduction

Conclusions

References

Tables

Figures

◀

▶

◀

▶

Back

Close

Full Screen / Esc

Printer-friendly Version

Interactive Discussion



- Follett, E. M. and Nepf, H. M.: Sediment patterns near a model patch of reedy emergent vegetation, *Geomorphology*, 179, 141–151, 2012. 607, 612
- Fonseca, M. and Cahalan, J.: A preliminary evaluation of wave attenuation by four species of seagrasses, *Estuar. Coast. Shelf Sci.*, 35, 565–576, 1992. 607
- 5 Friedrichs, M., Graf, G., and Springer, B.: Skimming flow induced over a simulated polychaete tube lawn at low population densities, *Mar. Ecol.-Prog. Ser.*, 192, 219–228, 2000. 603, 608
- Graf, G. and Rosenberg, R.: Bioresuspension and biodeposition: a review, *J. Marine Syst.*, 11, 269–278, 1997. 603
- Green, M. O.: Test of sediment initial-motion theories using irregular-wave field data, *Sedimentology*, 46, 427–441, 1999. 606
- 10 Houck, M. and Neill, R.: Plant fact sheet for black mangrove (*Avicennia germinans* (L.) L.), Tech. rep., USDA-Natural Resources Conservation Service, Louisiana Plant Materials Center, 2009. 603
- Infantes, E., Orfila, A., Simarro, G., Terrados, J., Luhar, M., and Nepf, H.: Effect of a sea-grass (*Posidonia oceanica*) meadow on wave propagation, *Mar. Ecol.-Prog. Ser.*, 456, 63–72, 2012. 607
- 15 Kobayashi, N., Raichle, A., and Asano, T.: Wave attenuation by vegetation, *J. Waterway, Port, Coastal, Ocean Eng.*, 119, 30–48, 1993. 607
- Komar, P. D. and Miller, M. C.: The threshold of sediment movement under oscillatory water waves, *J. Sediment. Petrol.*, 43, 1101–1110, 1973. 606, 613
- 20 LeHir, P., Monbet, Y., and Orvain, F.: Sediment erodability in sediment transport modelling: Can we account for biota effects?, *Cont. Shelf Res.*, 27, 1116–1142, 2007. 603
- Luckenbach, M.: Sediment stability around animal tubes: The roles of hydrodynamic processes and biotic activity, *Limnol. Oceanogr.*, 31, 779–787, 1986. 603
- 25 Madsen, J., Chambers, P., James, W., Koch, E., and Westlake, D.: The interaction between water movement, sediment dynamics and submersed macrophytes, *Hydrobiologia*, 444, 71–84, 2001. 603, 613, 614
- Maza, M., Lara, J., and Losada, I.: A coupler model of submerged vegetation under oscillatory flow using Navier-Stokes equations, *Coast. Eng.*, 80, 16–34, 2013. 607
- 30 Nepf, H.: Flow and transport in regions with aquatic vegetation, *Annu. Rev. Fluid Mech.*, 44, 123–142, 2012a. 606, 608
- Nepf, H.: Hydrodynamics of vegetated channels, *J. Hydraul. Res.*, 50, 262–279, 2012b. 606

---

## Observations of the effect of emergent vegetation

R. O. Tinoco and G. Coco

---

Title Page

Abstract

Introduction

Conclusions

References

Tables

Figures



Back

Close

Full Screen / Esc

Printer-friendly Version

Interactive Discussion



Nikora, V.: ydrodynamics of aquatic ecosystems: an interface between ecology, biomechanics and environmental fluid mechanics, *River Res. Appl.*, 26, 367–384, 2010. 603

Soulsby, R.: *Dynamics of marine sands*, Thomas Telford Publications, 1997. 604, 605, 606

Sumer, B., Chua, L., Cheng, N., and Fredsoe, J.: Influence of turbulence on bed load sediment transport, *J. Hydraul. Eng.*, 129, 585–596, 2003. 612

Tinoco, R. and Cowen, E.: The direct and indirect measurement of boundary stress and drag on individual and complex arrays of elements, *Exp. Fluids*, 54, 1–16, 2013. 610

VanHoey, G., Guilini, K., Rabaut, M., Vincx, M., and Degraer, S.: Ecological implications of the presence of the tube-building polychaete *Lanice conchilega* on soft-bottom benthic ecosystems, *Mar. Biol.*, 154, 1009–1019, 2008. 602

VanRijn, L.: Sediment transport, Part II: Suspended load transport, *J. Hydraul. Eng.*, 110, 1613–1641, 1984. 604, 606

Wallentinus, I. and Nyberg, C.: Introduced marine organisms as habitat modifiers, *Mar. Pollut. Bull.*, 55, 323–332, 2007. 602

Widdows, J. and Brinsley, M.: Impact of biotic and abiotic processes on sediment dynamics and the consequences to the structure and functioning of the intertidal zone, *J. Sea Res.*, 48, 143–156, 2002. 614

## Observations of the effect of emergent vegetation

R. O. Tinoco and G. Coco

Title Page

Abstract

Introduction

Conclusions

References

Tables

Figures

◀

▶

◀

▶

Back

Close

Full Screen / Esc

Printer-friendly Version

Interactive Discussion



**Table 1.** Relevant parameters for the studied arrays.

$n$ ( $m^{-2}$ )	$a$ ( $m^{-1}$ )	$\phi$	$\langle s \rangle / d$
0	–	–	–
25	0.5	0.008	4.45
150	3.0	0.047	1.70
250	5.0	0.079	1.40

**Table 2.** Wave parameters for all densities at locations  $x_c = 0$  m and  $x_c = 3$  m.

$n$ ( $\text{m}^{-2}$ )	$x_c = 0$ m				$x_c = 3$ m			
	$H_m$ (m)	$U_{w+}$ ( $\text{m s}^{-1}$ )	$U_{w-}$ ( $\text{m s}^{-1}$ )	$d_w$ (m)	$H_m$ (m)	$U_{w+}$ ( $\text{m s}^{-1}$ )	$U_{w-}$ ( $\text{m s}^{-1}$ )	$d_w$ (m)
0	0.013	0.076	-0.093	0.030	0.015	0.083	-0.098	0.033
0	0.029	0.143	-0.067	0.057	0.031	0.120	-0.162	0.048
0	0.047	0.228	-0.076	0.091	0.047	0.188	-0.127	0.075
0	0.062	0.289	-0.092	0.115	0.060	0.221	-0.198	0.088
0	0.079	0.304	-0.112	0.121	0.079	0.245	-0.245	0.098
25	0.014	-	-	-	-	-	-	-
25	0.031	0.128	-0.068	0.051	0.029	0.131	-0.047	0.052
25	0.050	0.224	-0.062	0.089	0.044	0.200	-0.084	0.079
25	0.068	0.293	-0.077	0.116	0.055	0.222	-0.163	0.088
25	0.078	0.313	-0.081	0.125	0.063	0.257	-0.171	0.102
150	0.012	0.068	-0.078	0.027	0.013	0.071	-0.086	0.028
150	0.029	0.141	-0.134	0.056	0.024	0.086	-0.076	0.034
150	0.047	0.233	-0.129	0.093	0.032	0.113	-0.098	0.045
150	0.064	0.288	-0.168	0.114	0.038	0.127	-0.126	0.050
150	0.070	0.289	-0.157	0.115	0.042	0.148	-0.137	0.059
250	0.015	0.047	-0.042	0.019	0.014	0.053	-0.040	0.021
250	0.031	0.106	-0.078	0.042	0.022	0.102	-0.038	0.041
250	0.047	0.214	-0.085	0.085	0.027	0.130	-0.053	0.052
250	0.062	0.259	-0.122	0.103	0.031	0.137	-0.082	0.055
250	0.078	0.291	-0.128	0.116	0.036	0.144	-0.101	0.057

## Observations of the effect of emergent vegetation

R. O. Tinoco and G. Coco

Title Page

Abstract

Introduction

Conclusions

References

Tables

Figures

◀

▶

◀

▶

Back

Close

Full Screen / Esc

Printer-friendly Version

Interactive Discussion



## Observations of the effect of emergent vegetation

R. O. Tinoco and G. Coco

**Table 3.** Measured critical velocities for currents,  $U_c$ , and critical orbital velocities,  $U_{wc}$ , according to the measurements of suspended sediment concentration at  $z = 0.05$  m for all densities.

$n$ ( $\text{m}^{-2}$ )	$U_c$ ( $\text{m s}^{-1}$ )	$U_{wc}$ ( $\text{m s}^{-1}$ )
250	0.080	0.063
150	0.096	0.071
25	0.111	0.131
0	0.163	0.120

Title Page

Abstract

Introduction

Conclusions

References

Tables

Figures

◀

▶

◀

▶

Back

Close

Full Screen / Esc

Printer-friendly Version

Interactive Discussion



## Observations of the effect of emergent vegetation

R. O. Tinoco and G. Coco

Title Page

Abstract

Introduction

Conclusions

References

Tables

Figures

◀

▶

◀

▶

Back

Close

Full Screen / Esc

Printer-friendly Version

Interactive Discussion



**Table 4.** Theoretical critical values for sediment motion (SM) and resuspension (*R*).

Criteria	$U_c$ ( $\text{m s}^{-1}$ )
van Rijn 1984 (SM)	0.297
Soulsby 1997 (SM)	0.259
Soulsby and Whitehouse 1997 (SM)	0.312
vanRijn 1984 ( <i>R</i> )	0.532
Soulsby 1997 ( <i>R</i> )	0.917

# ESURFD

1, 601–636, 2013

## Observations of the effect of emergent vegetation

R. O. Tinoco and G. Coco



**Fig. 1.** Species represented in the study. Black mangrove roots (left) and European fan worm (right). Pictures obtained from the USDA-NRCS and MESA websites, respectively.

Title Page

Abstract

Introduction

Conclusions

References

Tables

Figures

◀

▶

◀

▶

Back

Close

Full Screen / Esc

Printer-friendly Version

Interactive Discussion



**Observations of the  
effect of emergent  
vegetation**

R. O. Tinoco and G. Coco

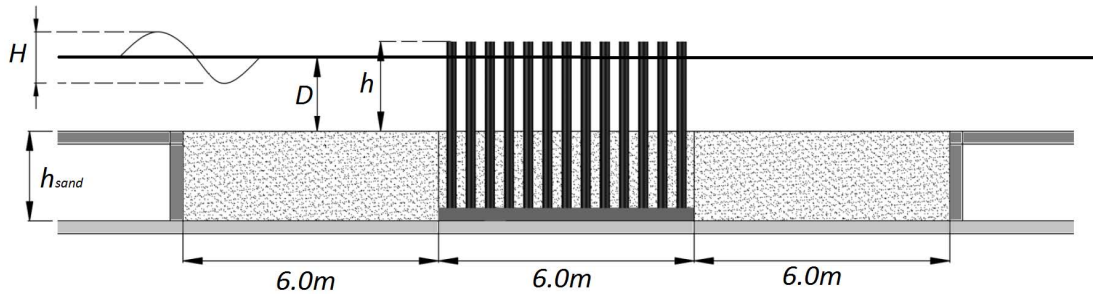


**Fig. 2.** Random array of emergent cylinders,  $d = 2.0$  cm, protruding  $h = 21$  cm above the sand bed. Water depth was set at  $D = 0.16$  m for all cases.

Title Page

Abstract

Introduction

Conclusions

References

Tables

Figures

◀

▶

◀

▶

Back

Close

Full Screen / Esc

Printer-friendly Version

Interactive Discussion



## Observations of the effect of emergent vegetation

R. O. Tinoco and G. Coco

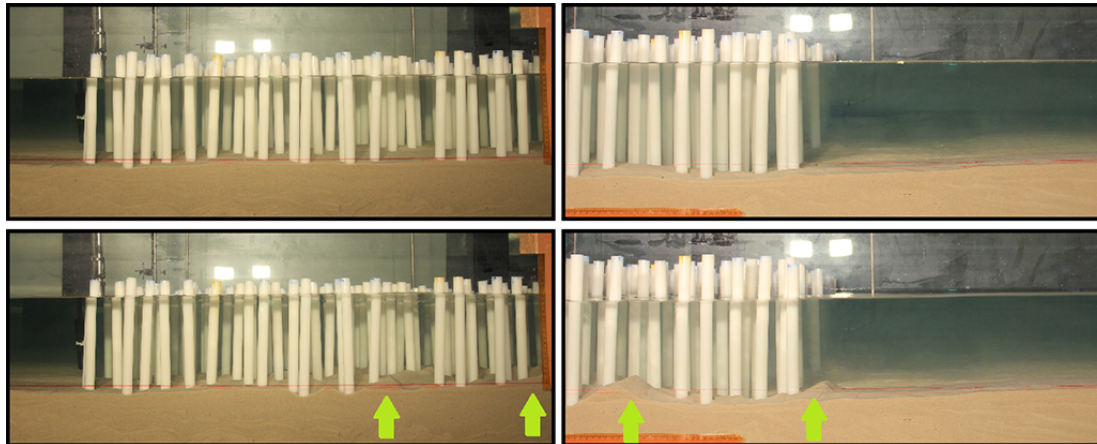


**Fig. 3.** Side view,  $n = 150 \text{ m}^{-2}$ , upstream (left) and downstream (right) edge of the array, before (up) and after (down) 5 min running at  $f_p = 30 \text{ Hz}$ . Notice the scour and bedforms forming within the array at the up- and downstream sections (as pointed by the green arrows).

Title Page

Abstract

Introduction

Conclusions

References

Tables

Figures

⏪

⏩

◀

▶

Back

Close

Full Screen / Esc

Printer-friendly Version

Interactive Discussion



**Observations of the  
effect of emergent  
vegetation**

R. O. Tinoco and G. Coco

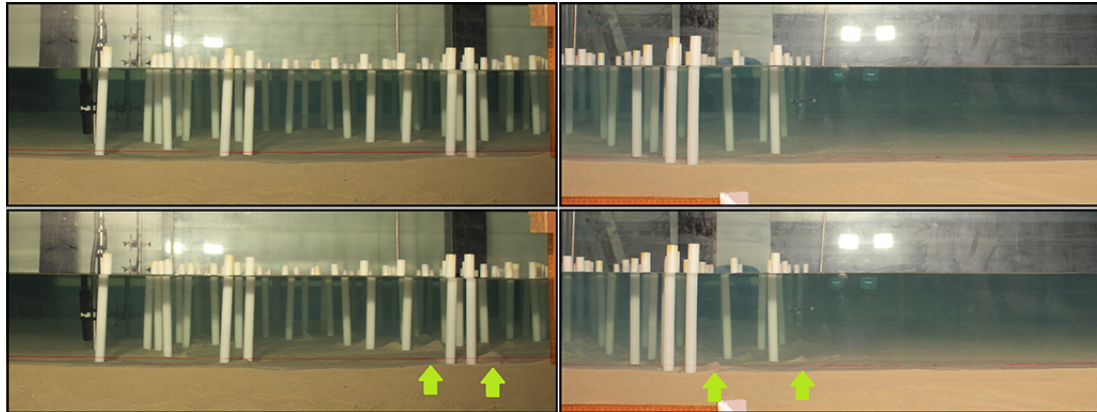


**Fig. 4.** Side view,  $n = 25 \text{ m}^{-2}$ , upstream (left) and downstream (right) edge of the array, before (up) and after (down) 5 min running at  $f_p = 30 \text{ Hz}$ . Notice the scour and bedforms forming within the array at the up- and downstream sections (as pointed by the green arrows).

Title Page

Abstract

Introduction

Conclusions

References

Tables

Figures

◀

▶

◀

▶

Back

Close

Full Screen / Esc

Printer-friendly Version

Interactive Discussion



## Observations of the effect of emergent vegetation

R. O. Tinoco and G. Coco

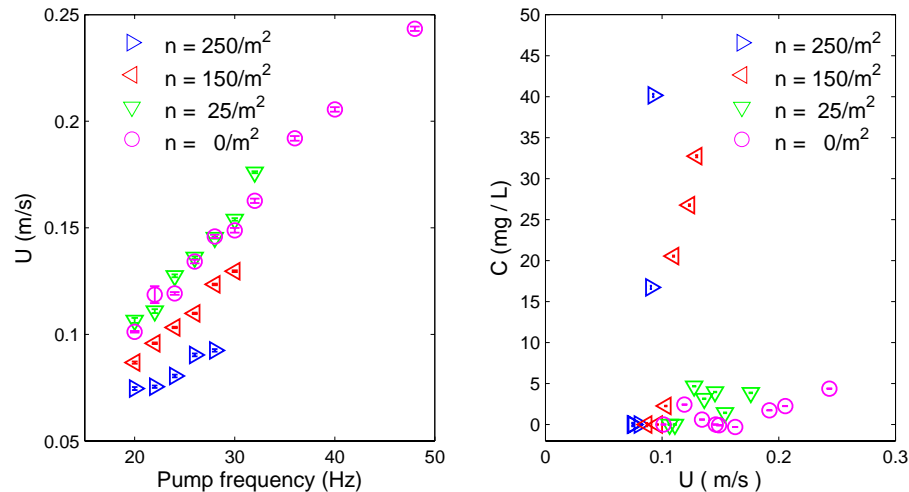


**Fig. 5.** Left: mean longitudinal,  $x$  velocities as a function of the pump frequency. Right: mean suspended sediment concentrations recorded at each velocity for all densities. Notice the range of velocities studied decreased for the denser cases to avoid large disruptions in the bed.

Title Page

Abstract

Introduction

Conclusions

References

Tables

Figures

◀

▶

◀

▶

Back

Close

Full Screen / Esc

Printer-friendly Version

Interactive Discussion



**Observations of the  
effect of emergent  
vegetation**

R. O. Tinoco and G. Coco

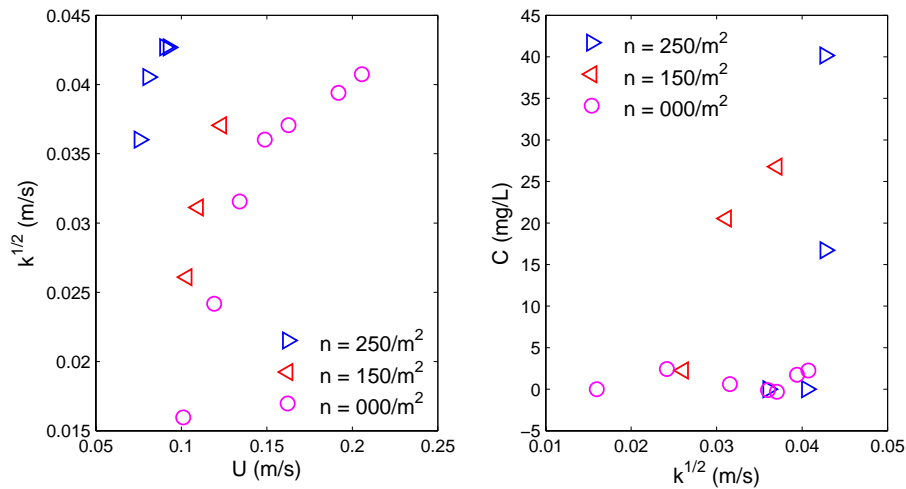


**Fig. 6.** Increase in turbulent kinetic energy,  $k$ , as a function of mean velocity  $U$  (left), and concentrations against  $k$  for all densities (right).

## Observations of the effect of emergent vegetation

R. O. Tinoco and G. Coco

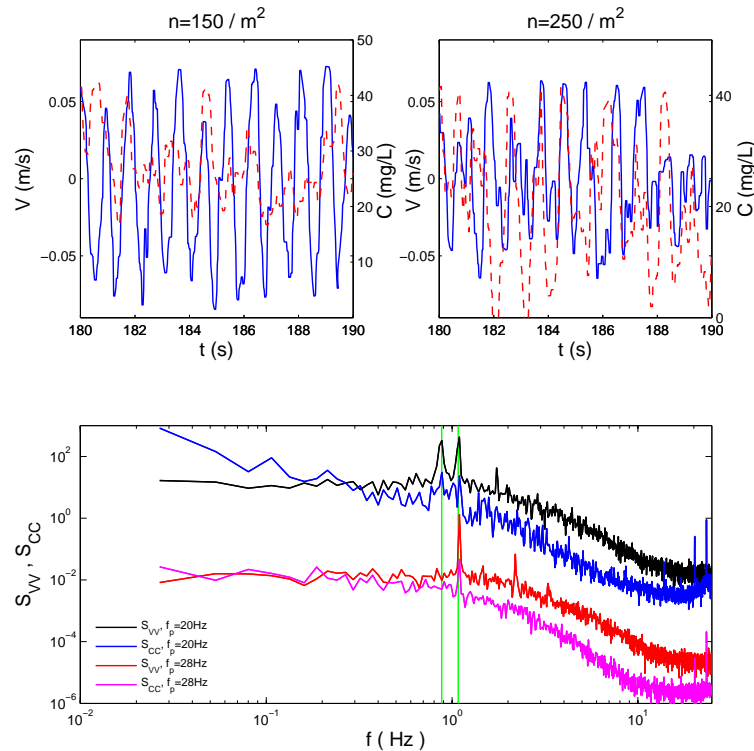


**Fig. 7.** Top: transversal velocity (blue solid line) and concentration (red dashed line) fluctuations due to transversal standing waves generated with increasing density. Bottom: velocity and concentration spectra for  $n = 250 \text{ m}^{-2}$ , at the minimum and maximum flow rates considered. Vertical green lines show the expected frequencies for modes 1 (0.88 Hz) and 2 (1.08 Hz) of the flume. Magnitudes of  $S_{VV}$  and  $S_{CC}$  have been multiplied by factors of 10 to improve visualization.

## Observations of the effect of emergent vegetation

R. O. Tinoco and G. Coco

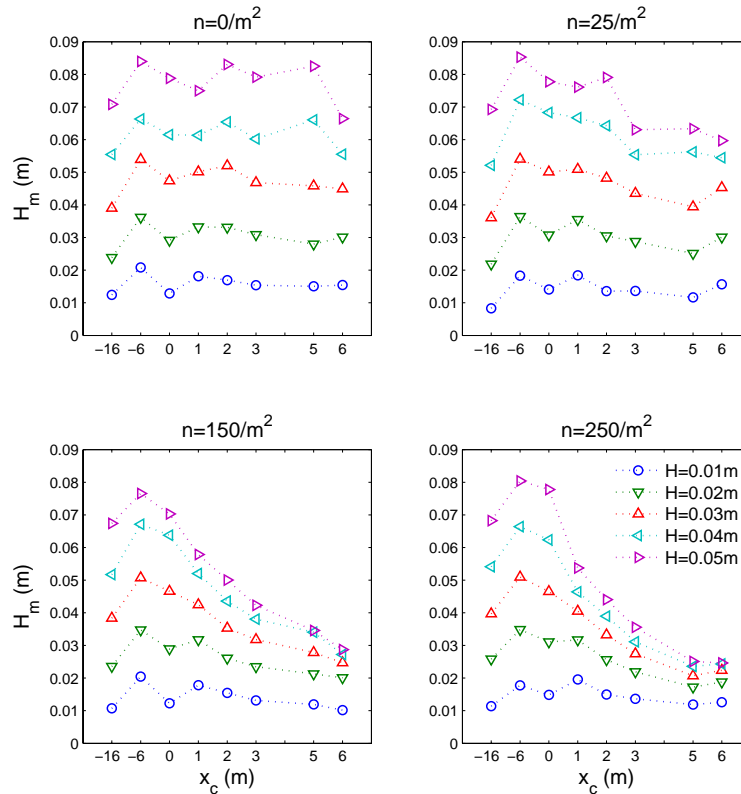


**Fig. 8.** Mean wave height,  $H_m$ , recorded along the flume, from the nearest sensor to the wave maker ( $x_c = -16$  m), to the beginning of the sand bed ( $x_c = -6$  m) to the end of the array ( $x_c = 6$  m). Notice negative  $x_c$  coordinates are not in scale.

## Observations of the effect of emergent vegetation

R. O. Tinoco and G. Coco

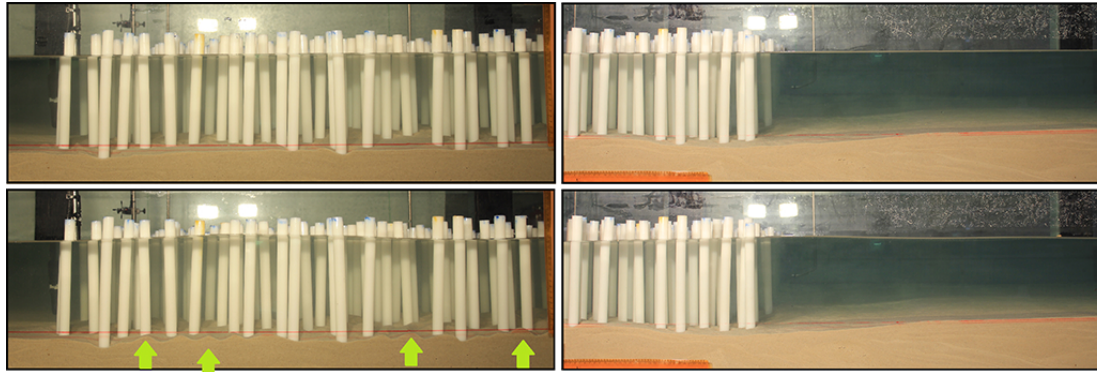


**Fig. 9.** Side view, upstream (left) and downstream (right) edge of the array, before (up) and after (down) 50 waves,  $H = 0.05$  m,  $T = 2.5$  s,  $n = 150$  m<sup>-2</sup>. Notice the scour and bedforms forming within the array at the upstream section (as pointed by the green arrows) while the downstream section remains unaltered.

Title Page

Abstract

Introduction

Conclusions

References

Tables

Figures

◀

▶

◀

▶

Back

Close

Full Screen / Esc

Printer-friendly Version

Interactive Discussion



**Observations of the effect of emergent vegetation**

R. O. Tinoco and G. Coco

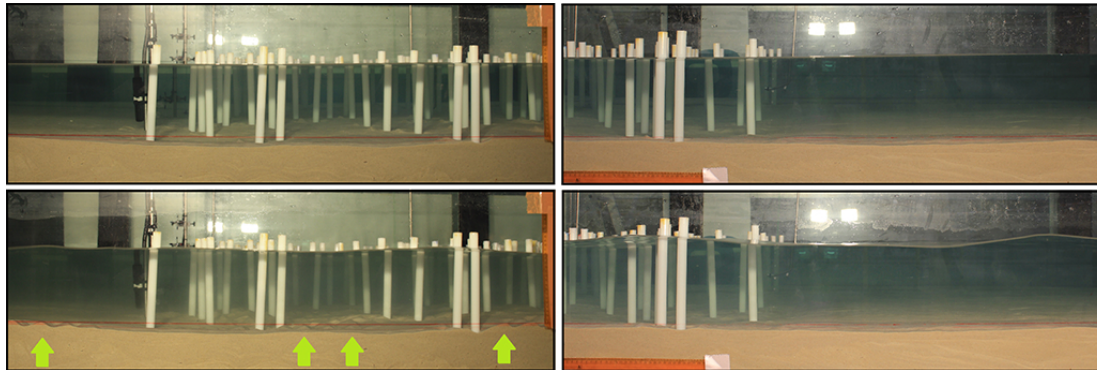


**Fig. 10.** Side view, upstream (left) and downstream (right) edge of the array, before (up) and after (down) 50 waves,  $H = 0.05$  m,  $T = 2.5$  s,  $n = 25$  m<sup>-2</sup>. Notice the scour and bedforms forming within the array at the upstream section (as pointed by the green arrows) while the downstream section remains unaltered.

Title Page

Abstract

Introduction

Conclusions

References

Tables

Figures

◀

▶

◀

▶

Back

Close

Full Screen / Esc

Printer-friendly Version

Interactive Discussion



## Observations of the effect of emergent vegetation

R. O. Tinoco and G. Coco

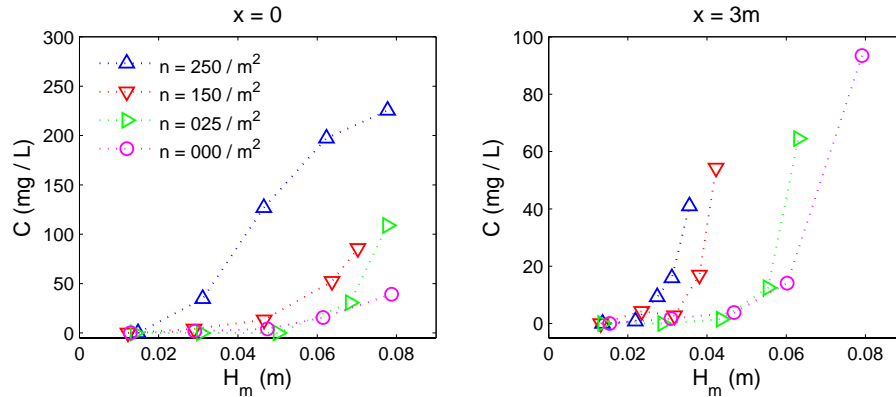


**Fig. 11.** Mean concentrations against measured mean wave heights for all densities at two instrumented locations. Notice the different vertical scales.

Title Page	
Abstract	Introduction
Conclusions	References
Tables	Figures
◀	▶
◀	▶
Back	Close
Full Screen / Esc	
Printer-friendly Version	
Interactive Discussion	



## Observations of the effect of emergent vegetation

R. O. Tinoco and G. Coco

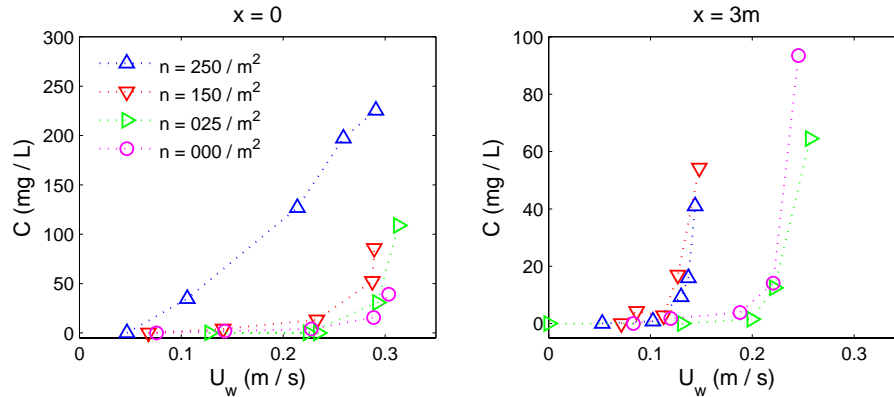


**Fig. 12.** Mean concentrations against measured near-bottom orbital speed for all densities at two instrumented locations. Notice the different vertical scales.

Title Page	
Abstract	Introduction
Conclusions	References
Tables	Figures
◀	▶
◀	▶
Back	Close
Full Screen / Esc	
Printer-friendly Version	
Interactive Discussion	



## Observations of the effect of emergent vegetation

R. O. Tinoco and G. Coco

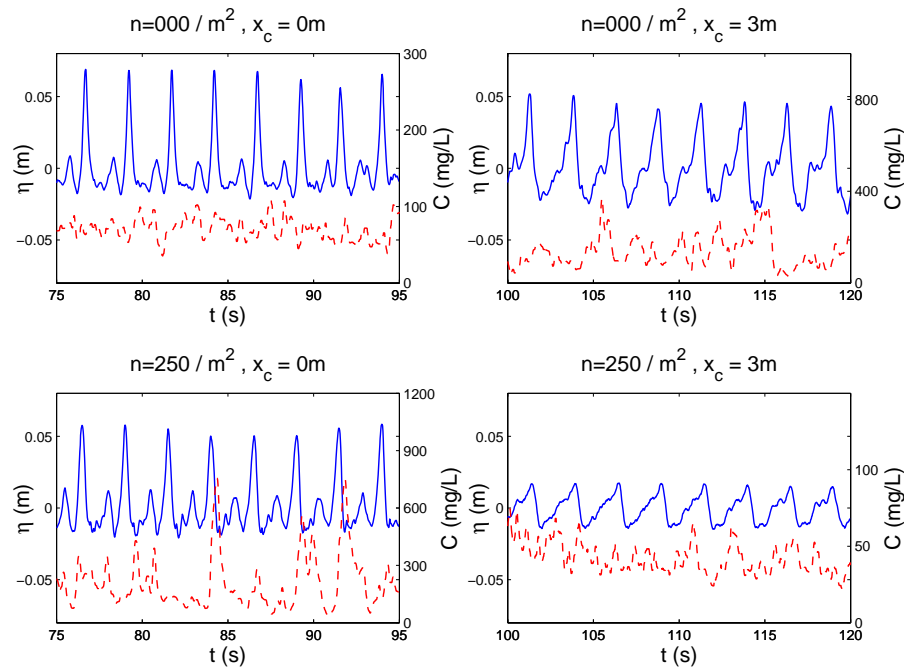


**Fig. 13.** Time series of free surface elevation (blue solid line) and concentration (red dashed line) for the non-populated (up) and densest (down) cases, at locations  $x_c = 0\text{ m}$  (left) and  $x_c = 3\text{ m}$  (right), for waves  $H = 0.05\text{ m}$ . Notice the scale for  $\eta$  is conserved in all figures, while the scale of  $C$  changes between figures.

**Observations of the  
effect of emergent  
vegetation**

R. O. Tinoco and G. Coco

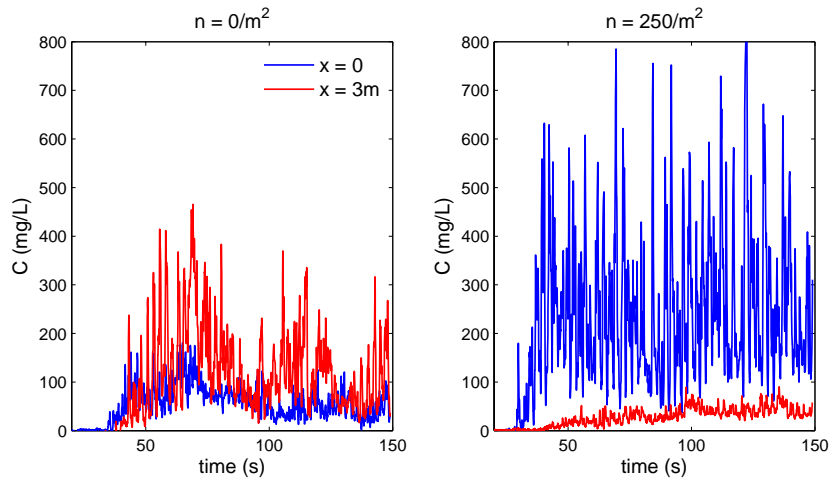


**Fig. 14.** Time series of suspended sediment concentration for the non-populated (left) and densest (right) cases, at locations  $x_c = 0$  m and  $x_c = 3$  m, for waves  $H = 0.05$  m.

Title Page

Abstract

Introduction

Conclusions

References

Tables

Figures

◀

▶

◀

▶

Back

Close

Full Screen / Esc

Printer-friendly Version

Interactive Discussion



## Observations of the effect of emergent vegetation

R. O. Tinoco and G. Coco

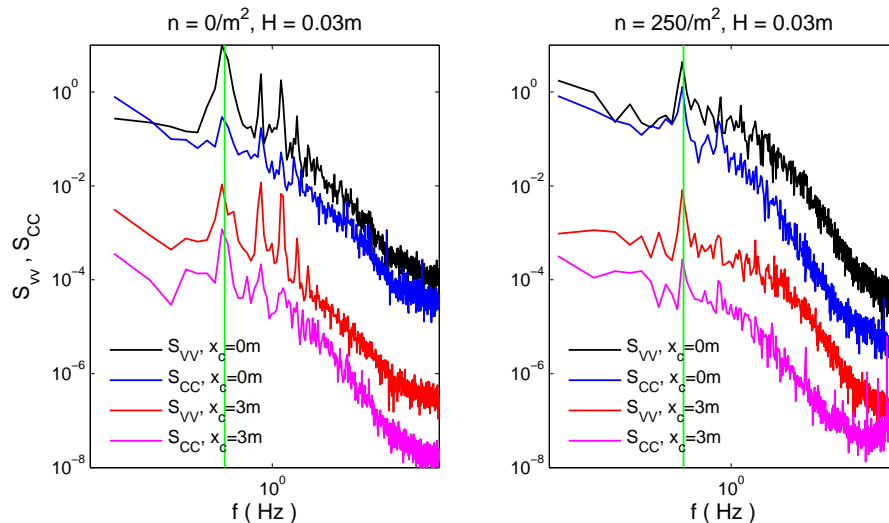


**Fig. 15.** Frequency spectra of transversal velocity and concentration for the cases  $n = 0 \text{ m}^{-2}$  (left) and  $n = 250 \text{ m}^{-2}$  (right), at longitudinal locations  $x_c = 0$  and  $x_c = 3$  m. Amplitudes multiplied by powers of 10 to improve visualization.

Title Page

Abstract

Introduction

Conclusions

References

Tables

Figures

◀

▶

◀

▶

Back

Close

Full Screen / Esc

Printer-friendly Version

Interactive Discussion

